CONF-8708117--4

CONF-8708117--4

DE87 013539

MAGNETIC DIFFUSE SCATTERING

J. W. Cable
Oak Ridge National Laboratory
Solid State Division
P.O. Box X
Oak Ridge, Tennessee 37831
U.S.A.

MAGNETIC DIFFUSE SCATTERING

J. W. Cable
Oak Ridge National Laboratory
Solid State Division
P.O. Box X
Oak Ridge, Tennessee 37831
U.S.A.

Abstract

The diffuse scattering of neutrons from magnetic materials provides unique and important information regarding the spatial correlations of the atoms and the spins. Such measurements have been extensively applied to magnetically ordered systems, such as the ferromagnetic binary alloys, for which the observed correlations describe the magnetic moment fluctuations associated with local environment effects. With the advent of polarization analysis, these techniques are increasingly being applied to study disordered paramagnetic systems such as the spin-glasses and the diluted magnetic semiconductors. The spin-pair correlations obtained are essential in understanding the exchange interactions of such systems. In this paper, we describe recent neutron diffuse scattering results on the atom-pair and spin-pair correlations in some of these disordered magnetic systems.

I. Introduction

While the Bragg scattering from a crystal is determined by the average scattering density and the average lattice, the diffuse scattering is related to the fluctuations of the scattering system from those averages. Both types of scattering are required for understanding the structure of real crystals, for which the diffuse scattering provides information on lattice distortions and on the spatial correlations of the atoms and the spins. In the case of magnetic materials, the nuclear and magnetic scattering often occurs in the same region of momentum space so that some separation technique is necessary. This separation method depends on the type of magnetic system being investigated. For a ferromagnet, Halperin and Johnson [1] showed that the magnetic scattering depends on both the initial spin state of the neutron and on the orientation of the magnetic moment relative to the momentum transfer vector, $\vec{Q}$. In particular, only that component of the moment perpendicular to $\vec{Q}$ is effective in magnetic scattering. This early theoretical result led to the development of two separation techniques for measurement of the magnetic diffuse scattering from ferromagnets. The first of these uses unpolarized neutrons and an applied magnetic field to extinguish the magnetic scattering by aligning the magnetic moments parallel to $\vec{Q}$. The second technique involves the use of polarized neutrons for which the nuclear and magnetic scattering amplitudes superpose. The scattered intensity therefore contains an additional nuclear-magnetic cross term which is readily separated by taking the difference between cross sections for incident beam polarizations parallel and antiparallel to the sample magnetization. This cross term is directly related to the effects of local environment on the magnetic moment distribution of the ferromagnetic alloy. Of course, neither of these techniques can be used for those magnetic materials, such as the antiferromagnets and paramagnets, for which the magnetization can not be controlled by an external magnetic field. Polarization analysis has become the standard separation technique for such systems. Excellent reviews [2-4] are available which cover the magnetic diffuse scattering from ferromagnets and antiferromagnets. In this paper, we concentrate on the diffuse scattering from paramagnetic systems. This is a well-established area of research with a theoretical basis extending back to Halperin and Johnson [1] in 1939 and with the first neutron experiments performed by Shull, Strauser, and Wollan [5] in 1951. No survey of the vast literature on this subject is attempted; instead the techniques and type of results obtained are illustrated by presentation of a few recent studies carried out at Oak Ridge.

II. Diffuse Scattering from Cu-Mn Alloys

The complicated magnetic behavior of Cu-Mn alloys has attracted considerable attention for a long time [6]. The Cu-rich alloys exhibit typical spin glass behavior in which the spins apparently freeze in random orientations below a concentration-dependent freezing temperature, T_f. The magnetic susceptibility is strongly dependent on heat treatment which suggests the presence of competing, short-range interactions between the Mn spins. Many neutron diffuse scattering studies [7-21] have been directed toward the determination of the spin-pair correlations that result from those interactions. In this fcc alloy, some degree of atomic short range order (ASRO) is always present and, unfortunately, the diffuse scattering arising from this ASRO superposes on the magnetic diffuse scattering over a large concentration region. This circumstance led to conflicting conclusions from some of the early neutron studies, but this has now been sorted out by use of polarization analysis and single crystal samples. The general features of the diffuse scattering from Cu-Mn alloys are illustrated by figure 1 which shows isointensity contours in a [001] reciprocal lattice plane for a Cu-35% Mn alloy. These room temperature data were taken on the WAND spectrometer at Oak Ridge which uses an incident neutron energy of 35 mev with no energy analysis of the scattered beam. Within the region covered by this scan, the allowed fundamental Bragg reflections are (200), (400), and (420). These reflections appear in the figure with intensities that are off-scale and with spurious, comet-like tails directed back toward the origin along the scattering arc. The diffuse scattering appears in the diffuse peaks centered at (1 1/2 0) type positions. The symmetry of this diffuse scattering distribution repeats in each Brillouin zone, but there is more intensity in the inner zones because of a superposition of the nuclear and magnetic scattering and the form factor dependence of the latter.

In favorable cases, a separation of this nuclear and magnetic scattering can be accomplished by taking temperature differences, but the best method is by polarization analysis. This technique [22] employs an incident neutron beam polarized in the (+) direction and an analyzer-detector system that accepts neutrons only in the (+) spin state. It is then possible to measure cross sections for (+ +), (- -), (+ -) and (- +) scattering by various on-off combinations of π spin flippers located before and after the sample. If the experiment is arranged with a guide field at the sample which maintains the

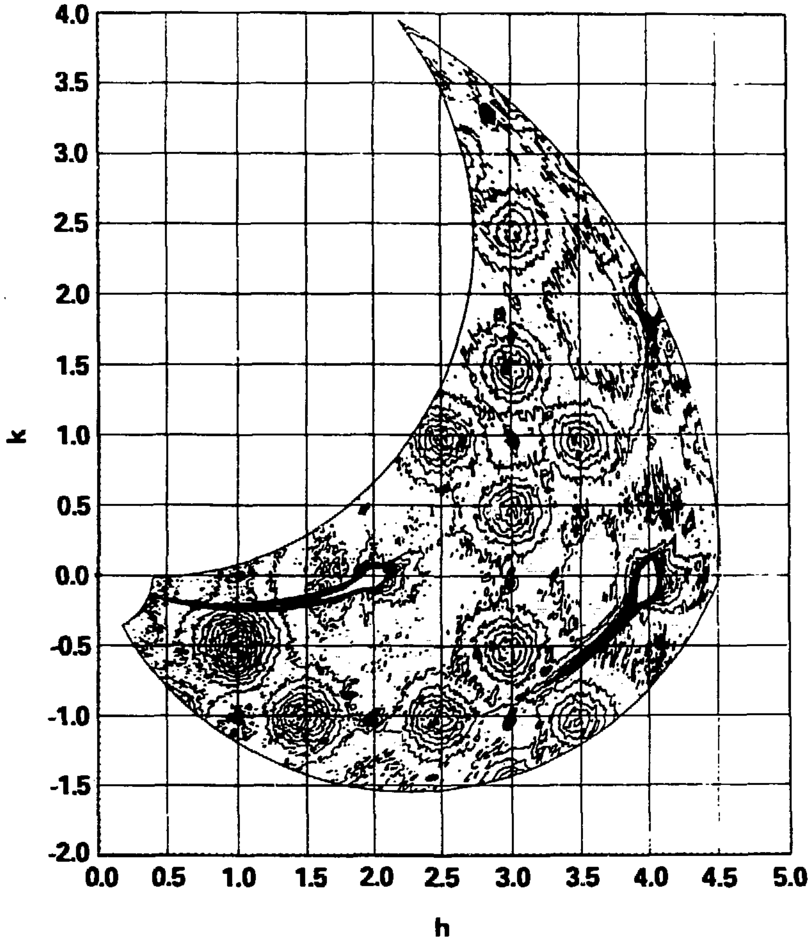

Figure 1. Isointensity contours for an annealed Cu-35% Mn alloy at 295 K.

neutron polarization parallel to $\vec{Q}$, then the nuclear scattering is non-spin-flip, (+ +) or (- -), while the magnetic scattering undergoes a spin-flip, (- +) or (+ -).

The non-spin-flip, or nuclear, cross section is given by

$$\frac{d\sigma^{++}}{d\Omega}(\vec{Q}) = c(1-c)(b_i-b_h)^2\ S(\vec{Q}) \tag{1}$$

where

$$S(\vec{Q}) = \sum_{\vec{R}} e^{i\vec{Q}\cdot\vec{R}}\ \alpha(\vec{R}) \tag{2}$$

in which b_i and b_h are the impurity and host nuclear scattering amplitudes, c is the impurity concentration and the $\alpha(\vec{R})$ are the ASRO parameters. If p_n^+ is defined as a site occupation operator that counts the number (either 0 or 1) of impurity atoms at the lattice site $\vec{n}$, then

$$c(1-c)\ \alpha(\vec{R}) = \langle (p_{\vec{n}+\vec{R}} - c)(p_{\vec{n}} - c) \rangle \tag{3}$$

where the angular brackets denote a configurational average. Thus, $\alpha(\vec{R})$ describes the spatial correlation of site occupation fluctuations from the average.

The neutron scattering cross section from an exchange coupled spin system is the Fourier transform of a time-dependent spin-pair correlation. Diffuse scattering experiments are ususally designed for quasi-elastic measurements which determine the static correlation for short times. Within the quasi-elastic approximation, the spin-flip, or magnetic, cross section for such a paramagnetic system can be written as

$$\frac{d\sigma^{-+}}{d\Omega}(\vec{Q}) = \left(\frac{e^2\gamma}{mc^2}\right)^2 f^2(Q) \sum_{\alpha\beta}(\delta_{\alpha\beta} - \hat{Q}_\alpha\hat{Q}_\beta) \sum_{R} e^{i\vec{Q}\cdot\vec{R}} \langle S^{\alpha}_{\vec{n}+\vec{R}}\, S^{\beta}_{\vec{n}} \rangle , \tag{4}$$

where α and β are Cartesian coordinates, $\hat{Q}_\alpha$ and $\hat{Q}_\beta$ are direction cosines of $\vec{Q}$ and $\langle S^{\alpha}_{\vec{n}+\vec{R}}\, S^{\beta}_{\vec{n}} \rangle$ is the configurationally averaged spin-pair correlation. Two conditions are required for this approximation to be valid: (1) the energy window of the analyzer-detector system must be wide enough to integrate over all energy transfers of the spin system, and (2) the incident energy must be sufficiently high that this integration is accomplished at nearly constant

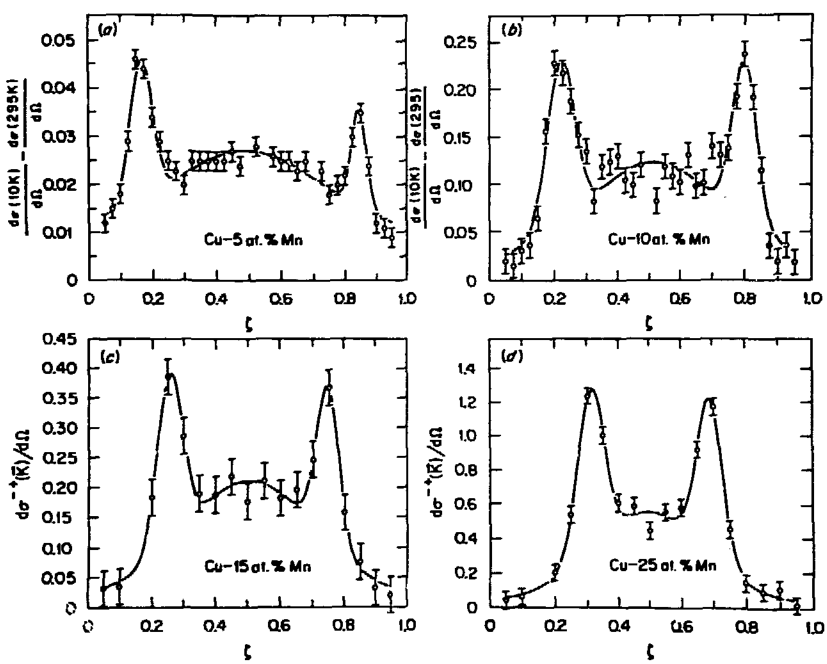

Figure 2. Magnetic diffuse scattering cross sections for Cu-Mn alloys along the [1 ζ 0] direction. Temperature difference data are shown in (a) and (b), while polarization analysis data for 10 K are given in (c) and (d).

$\vec{Q}$. If these conditions are not satisfied, then the static spin-pair correlations can only be determined by measurement of the full $S(\vec{Q},\omega)$ followed by an ω integration at constant $\vec{Q}$.

The magnetic diffuse scattering observed [19] for Cu-Mn alloys is shown in figure 2. These are data obtained with a triple-axis spectrometer set for elastic scattering and with the nuclear-magnetic separation achieved by the temperature difference method for (a) and (b) and by polarization analysis for (c) and (d). These data show two quite distinct types of magnetic short range order (MSRO). The broad diffuse peaks at (1 ½ 0) arise from a net ferromagnetic spin correlation that is directly associated with the ASRO. The relatively sharp, but still diffuse, peaks at (1, ½ ± δ, 0) result from an antiferromagnetic spin correlation which takes the form of an incommensurate long period modulation. The modulation wavelength varies linearly with Mn concention in such a manner that δ approaches zero at 50% Mn. This long period modulation has been attributed to an RKKY interaction between the Mn spins through the conduction electrons [17,19]. In this model, δ is determined by a wavevector connecting approximately flat regions of the Fermi surface.

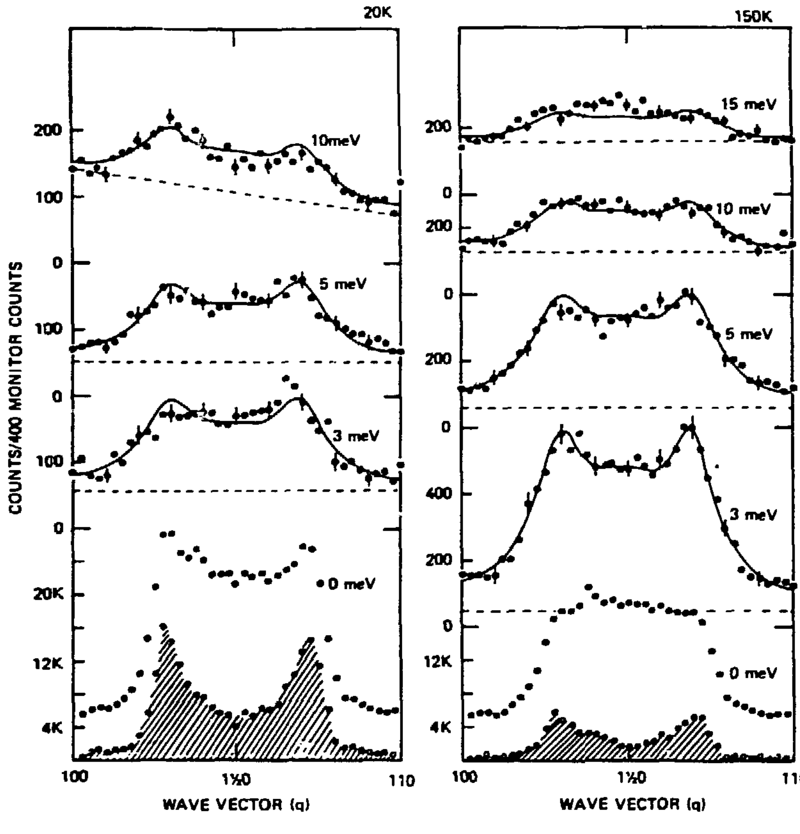

Figure 3. Constant energy scans along [1 ζ 0] for a Cu-21% Mn alloy at 20 K and 150 K (T_f = 90 K). The shaded areas represent magnetic scattering as obtained by the temperature difference method.

The microscopic spin structure that emerges from these studies is that of small ferromagnetically correlated regions homogeneously coexisting with the larger antiferromagnetic modulated regions. The spin dynamics associated with the ferromagnetic correlations was thoroughly studied by Murani [23-30] who found a wide spectral distribution of relaxation times evolving continuously with temperature. We [31] studied the spin dynamics of the antiferromagnetic correlations to better understand the interactions within and between these two types of MSRO regions. Figure 3 shows constant energy scans in the (1 1/2 0) region for a Cu-21% Mn alloy at temperatures above and below the spin glass freezing temperature ($T_f \approx 90$ K). These are unpolarized-beam triple-axis measurements with the final energy fixed at 13.8 mev and with an energy resolution of 1.2 mev FWHM at zero energy transfer. The intense peak at T = 20 K and $\Delta E = 0$ mev is a superposition of the MSRO peaks and the broad ASRO peak centered at (1 1/2 0). The open data points and the shaded area represent an approximation to the magnetic diffuse scattering as obtained by the temperature difference method (20 K - 290 K). This agrees well with the earlier measurements of figure 2. Even though $T \ll T_f$, inelastic scattering is observed with energy transfers up to 10 mev and with the same peak positions as for the elastic scattering. Comparison of the 20 K and 150 K panels shows an intensity shift from elastic to inelastic scattering with increasing T. This continues until all of the scattering is inelastic at 290 K under the energy resolution condition of this experiment. The curves in figure 3 were fitted by assuming Lorentzian line shapes in both $\vec{Q}$ and ω. The inverse correlation length is observed to be temperature independent suggesting spin clusters that maintain approximately the same dimensions over the temperature interval from 20 K to 290 K. This study shows that the composite ferro-antiferromagnetic clusters maintain their spatial correlations while undergoing an orientational fluctuation in time. This is interesting physics, but for our purpose here, it serves to demonstrate that the inherent inelasticity of paramagnetic scattering can become a problem in attempted studies of static spin correlations. The validity of the quasi-elastic approximation must be carefully considered for each experiment.

III. Diffuse Scattering From Ni-Mn Alloys

The magnetic behavior of Ni-Mn alloys is also dominated by the presence of competing interactions, but the holes in the Ni d-band now allow for magnetic moments on the Ni sites. The Ni-rich alloys are ferromagnetic and exhibit a remarkable dependence of magnetization on both concentration and heat treatment. Ferromagnetism is retained to about 40% Mn for annealed alloys but only to 24% Mn for quenched alloys [32,33]. The overall behavior can be explained by a molecular field model which assumes nearest-neighbor exchange interactions that are antiferromagnetic for Mn-Mn pairs and ferromagnetic for Ni-Ni and Ni-Mn pairs. The alignment of the magnetic moment at a given Mn site then depends on the net effective field exerted by the nearest-neighbor environment of that site. Spin-reversal [34] and canted-spin [35] models have been suggested and either will reproduce the concentration dependence of the magnetization with properly selected parameters.

These models gain support from polarized-neutron diffuse scattering measurements [36] which show a pronounced local environment effect that is negative for first neighbors and positive for second neighbors. Also, NMR measurements

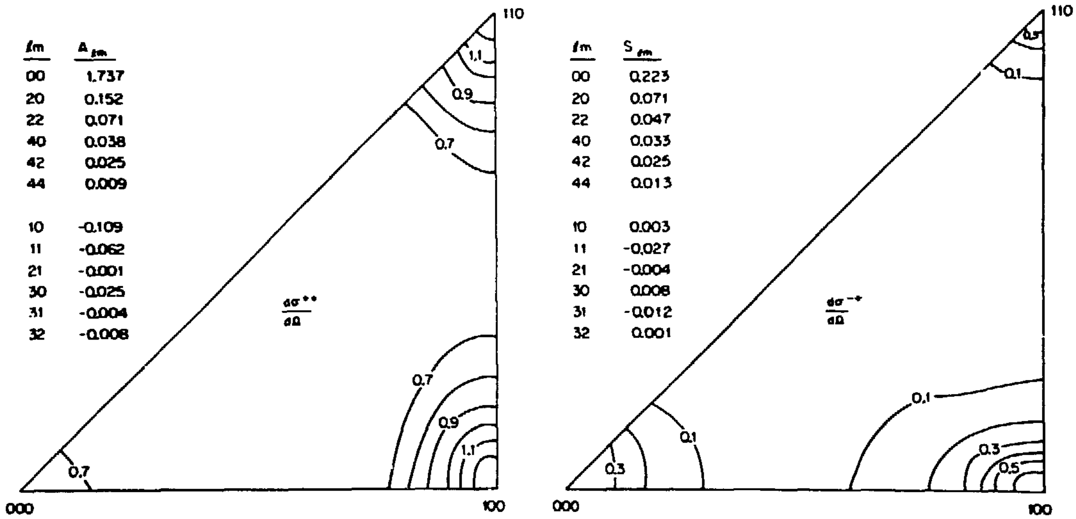

Figure 4. Contours of equal cross section for non-spin-flip (left) and spin-flip (right) scattering from a Ni-24% Mn alloy. Contours are in units of barns-steradian^{-1} - atom^{-1}. The $A_{\ell m}$ and $S_{\ell m}$ are two dimensional Fourier coefficients obtained from these data (see text).

[37] show a hyperfine field distribution at ^{55}Mn sites corresponding to three different types of Mn atoms. For quenched alloys, these competing interactions tend to cancel in the 24% Mn region where ferromagnetism no longer exists. Just below 24% Mn reentrant spin-glass behavior is observed [38-40]. The reentrant state appears to be a mixed state with both a spontaneous ferromagnetic moment and spin glass characteristics. This mixed state interpretation is supported by inelastic neutron measurements [41] on a 22% Mn alloy which show long wavelength spin waves present both above and below the reentrant state phase boundary. We recently completed a polarization analysis study [42] of the atom-pair and spin-pair correlations in this reentrant state region. Diffuse scattering results for a Ni-24% Mn alloy are given in figure 4 where contours of equal cross section are shown on the left for non-spin-flip scattering and on the right for spin-flip scattering. The nuclear scattering exhibits diffuse peaks at (100) and (110) which are associated with ASRO of the Cu_3Au type. These data were Fourier transformed to obtain the two dimensional Fourier coefficients listed alongside the figure. These are related to the three dimensional $\alpha(\vec{R})$ by

$$A_{\ell m} = \sum_{n} \alpha_{\ell mn} \ . \qquad (5)$$

Here, the atomic positions are given by

$$\vec{R} = 1/2 \ (\ell \vec{a}_1 + m\vec{a}_2 + n\vec{a}_3) \qquad (6)$$

where ℓ, m, and n are integers and $(\ell + m + n)$ is even in this fcc lattice.

The $A_{\ell m}$ have significant magnitudes out to A_{44} which contains contributions from the $\alpha_{\ell mn}$ out to at least 16 or 18 shells. With ASRO to such large distances, there is insufficient information to obtain a unique solution for the even shell $\alpha_{\ell mn}$. However, a reasonable solution can be obtained by setting all $\alpha_{\ell mn}$ beyond the 18th shell to zero and by constraining the $\alpha_{\ell mn}$ to decrease with increasing R. The $\alpha_{\ell mn}$ obtained with these restrictions show a preference for unlike odd-shell neighbors and like even-shell neighbors in accordance with the Cu_3Au type of ASRO.

The spin-flip cross section in figure 4 shows similar features with diffuse peaks at (000), (100), and (110). In this experiment, the applied magnetic field (which is parallel to $\vec{Q}$) defines the z axis of the spin system. Under these conditions, only the transverse spin components are observed so that the Fourier coefficients listed in the figure are given by

$$S_{\ell m} = \sum_n S_{\ell mn} \tag{7}$$

where the MSRO parameter is

$$S_{\ell mn} = \langle S^x_{\vec{n}+\vec{R}} \, S^x_{\vec{n}} \rangle \, . \tag{8}$$

Three dimensional $S_{\ell mn}$ were obtained by using the same constraints as those placed on the $\alpha_{\ell mn}$. These are positive for the even-shells and small but slightly negative for the first two odd-shells. This same alternating sequence was previously observed [36] for the longitudinal spin correlations, which suggests that spin-canting may be the correct model for these alloys.

IV. Diffuse Scattering From Au-Fe Alloys

The magnetic phase diagram of AuFe alloys exhibits a critical concentration, c_0, for the onset of ferromagnetism near 16 at % Fe. At concentrations below c_0, there is a single boundary between paramagnetic and spin-glass phases, while above c_0, there is a double transition with a reentrant spin-glass phase [43,44]. It is generally accepted that this behavior is associated with ferromagnetic spin clusters, but there is considerable current controversy regarding the nature and interaction of these clusters near c_0 [45-47]. Early interpretations of the double transition were based on a percolation model with ferromagnetism associated with the infinite cluster and spin-glass behavior attributed to coexistent finite clusters [43,44]. More recently, Mössbauer data [48-50], which show a canting of the moments away from the applied field direction in the reentrant phase, have been interpreted in terms of the mean field model of Gabay and Toulouse [51]. This model is characterized by the coexistence of spontaneous ferromagnetism with spin-glass ordering of the transverse spin components.

X-ray diffuse scattering from quenched AuFe alloys in this critical composition region shows diffuse streaks in <210> directions [52]. These are attributed to a tendency toward the formation of Fe atom platelets in {420} planes which are approximately two atomic layers thick and 30 Å in diameter. The authors speculate that the spins in these platelets are ferromagnetically aligned with the moments constrained to lie within the {420} planes by shape anisotropy. Beck [53] reviews the experimental evidence and concludes that

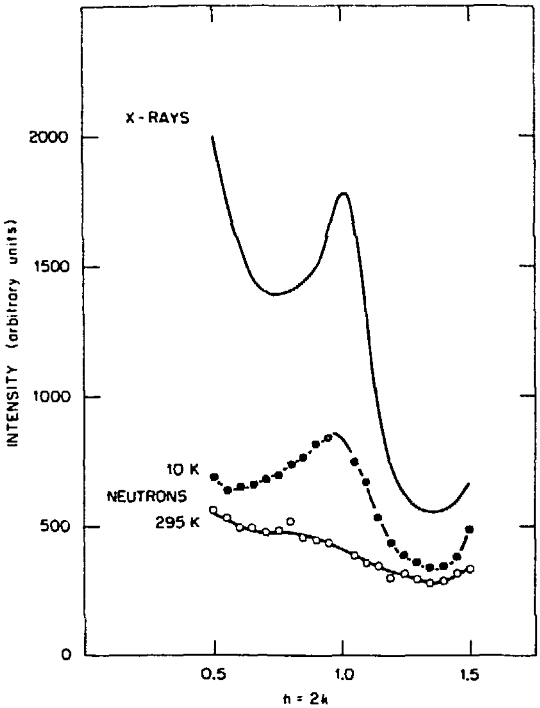

Figure 5. A comparison of the diffuse scattering in the [210] direction of x-rays [52] and of neutrons [54] from a Au-15% Fe alloy.

the magnetic behavior of these alloys is consistent with the presence of such platelets with the orientation of the platelet moment at low temperatures being determined by a quasi-random local anisotropy.

In view of the uncertainties in the nature of the spin correlations in these alloys, we decided to investigate these by neutron diffuse scattering [54]. Unpolarized neutrons were used and no separation of the nuclear and magnetic scattering was made. However, the expected Laue monotonic cross section for magnetic scattering is 109 f (Q) mb/atom compared to only 5 mb/atom for the nuclear scattering. In essence then, the neutron cross section measures only the MSRO while the x-ray scattering determines the ASRO. A comparison of the x-ray and neutron results is given in figure 5 which shows the intensity measured along the [210] direction by the two techniques. The upper curve is a sketch of the x-ray data taken from reference [52], and the lower curves represent the neutron data at temperatures of 10 K and 295 K. The magnetic neutron scattering is clearly temperature dependent and peaks at (1 ½ 0) just as does the nuclear x-ray scattering. The similarity between the x-ray and neutron data is even more pronounced in a two dimensional representation as given in figure 6 which shows isointensity contours for the T = 10 K neutron data. Just as for the x-ray case, there is diffuse scattering around the origin and a diffuse streak in the [210] direction. In addition, the Lorentzian half-width of the diffuse streak transverse to [210] is the same

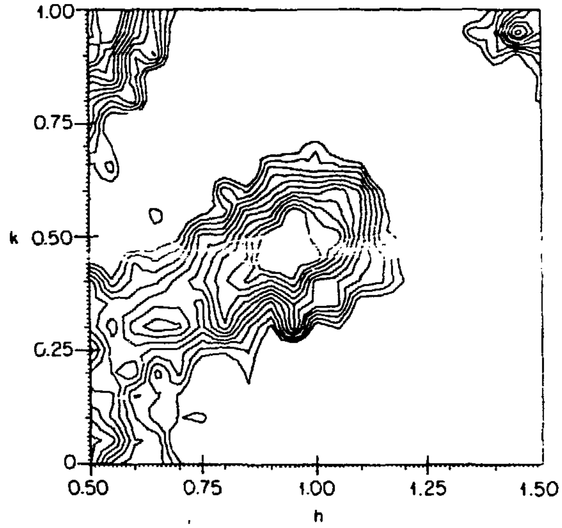

Figure 6. Isointensity contours for a Au-15% Fe alloy at 10 K. The contours are equally spaced from 550 to 800 counts.

(0.125 $2\pi/a$) as that measured with x-rays. This similarity between the spin-pair and atom-pair correlations is a consequence of the fact that only the Fe atoms have spins. The spin-pair correlation is then

$$\langle S^{\alpha}_{\vec{R}}\, S^{\beta}_{\vec{n}+\vec{R}} \rangle = \langle p_{\vec{R}}\, S^{\alpha}_{Fe}(\vec{R})\, p_{\vec{n}+\vec{R}}\, S^{\beta}_{Fe}(\vec{n}+\vec{R})\rangle \tag{9}$$

and the Fe-Fe atom-pair correlation is

$$\langle p_{\vec{R}}\, p_{\vec{n}+\vec{R}} \rangle = c^2 + c(1-c)\, \alpha(\vec{R}). \tag{10}$$

If these correlations are separable, then

$$\langle S^{\alpha}_{\vec{R}}\, S^{\beta}_{\vec{n}+\vec{R}} \rangle = [c^2 + c(1-c)\alpha(\vec{R})]\langle S^{\alpha}_{Fe}(\vec{R})\, S^{\beta}_{Fe}(\vec{n}+\vec{R})\rangle \tag{11}$$

and a ferromagnetic Fe-Fe correlation will produce the observed low temperature features of diffuse scattering at both (000) and (1 ½ 0).

Additional information about the nature of these correlations is gained from the effects of lattice distortions on the scattered intensity. This is quite pronounced in the x-ray case for which there is an asymmetry in the streak intensity around the fundamental reciprocal lattice points such that intensity is only observed for those streaks directed back toward the origin. This is expected if those atoms within the platelets have both a smaller scattering amplitude and a smaller atomic size than the average atom. In the Fe atom platelet model proposed by Dartyge et. al. [52], it is the intersection and superposition of intensity for four such streaks [originating from (000), (200), (111), and $11\bar{1}$)] that produces the (1 ½ 0) diffuse peak. However, the reverse situation should apply to the neutron data; i.e., the smaller Fe atoms have the larger magnetic scattering amplitudes and diffuse streaks due to ferromagnetic platelets should point away from the origin. In that event, there should be no intersection of streaks and no diffuse peak at (1 ½ 0). Therefore, scattering from independent ferromagnetic platelets cannot produce the observed neutron data which instead requires some type of damped periodicity in the direction normal to the platelets. We conclude that there is a tendency toward the formation of Fe platelets in {420} planes; these are not randomly distributed but have a quasi-periodicity in directions normal to the platelets. The MSRO is attributed to ferromagnetic spin correlations within these platelets but with a range that extends beyond that of the ASRO at low temperatures.

Conclusions

Neutron diffuse scattering measurements have furnished a wealth of information on the magnetic moment fluctuations in magnetic materials. Most of the experimental studies have dealt with the ferromagnetic substitutional alloys, and for these, the observed magnetic moment spatial distributions have strongly impacted theoretical developments. The average magnetic moments of the constituents are now successfully calculated by the single-site CPA method and some of the observed local environment effects are being obtained by cluster CPA calculations [55,56]. Such direct contact with theory is not yet possible for studies of paramagnetic systems. Nevertheless, much of the experimental activity has recently shifted into this area where spin correlation information is needed to understand the behavior of new materials. Currently, these new materials include the reentrant spin glasses, the diluted magnetic semiconductors, and the high temperature superconductors. There will undoubtedly be other classes of materials for future studies. Such studies will produce even more detailed information than is presently obtained because of improvements in detection and data-handling systems, better polarized beam methods, and the increasing availability of single crystal samples.

Acknowledgments

This research was supported by the Division of Materials Sciences, U. S. Department of Energy under contract DE-AC05-84OR21400 with Martin Marietta Energy Systems, Inc.

References

1. Halperin, O. and Johnson, M. H.: Phys. Rev., 1939, 55, 898
2. Low, G. G.: Advances in Phys., 1969, 18, 371
3. Hicks, T. J.: "Treatise on Materials Science and Technology," Vol. 15, Neutron Scattering, Academic Press, New York, 1979, p. 337
4. Rainford, B. D.: J. de Phys., 1982, 43, C7-33
5. Shull, C. G., Strauser, W. A., and Wollan, E. O.: Phys. Rev., 1951, 83, 333
6. Beck, P. A.: Prog. Materials Science, 1978, 23, 1
7. Meneghetti, D. and Sidhu, S. S.: Phys. Rev., 1957, 105, 130
8. Wells, P. and Smith, J. H.: J. Phys. F: Metal Phys., 1971, 1, 763
9. Sato, H., Werner, S. A., and Yessik, M.: AIP Conf. Proc., 1971, 5, 508
10. Werner, S. A., Sato, H., and Yessik, M.: AIP Conf. Proc., 1972, 10, 679
11. Ahmed, N. and Hicks, T. J.: Solid State Commun., 1974, 15, 415
12. Ahmed, N. and Hicks, T. J.: J. Phys. F: Met. Phys., 1975, 5, 2168
13. Davis, J. R. and Hicks, T. J.: J. Phys. F: Met. Phys., 1979, 9, 753
14. Davis, J. R., Burke, S. K., and Rainford, B. D.: J. Magn. Magn. Mater., 1980, 15-18, 151
15. Werner, S. A. and Cable, J. W.: J. Appl. Phys., 1981, 52, 1757
16. Cable, J. W., Werner, S. A., Felcher, G. P., and Wakabayashi, N.: Phys. Rev. Lett., 1982, 49, 829
17. Harders, T. M. and Wells, P.: J. Phys. F: Met. Phys., 1983, 13, 1017
18. Harders, T. M., Hicks, T. J., and Smith, J. H.: J. Phys. F: Met. Phys., 1983, 13, 1263
19. Cable, J. W., Werner, S. A., Felcher, G. P., and Wakabayashi, N.: Phys. Rev. B, 1984, 29, 1268
20. Werner, S. A. Rhyne, J. J., and Gotaas, J. A.: Solid State Commun., 1985, 56, 457
21. Gotaas, J. A., Rhyne, J. J., and Werner, S. A.: J. Appl. Phys., 1985, 57, 3404
22. Moon, R. M., Riste, T., and Koehler, W. C.: Phys. Rev., 1969, 181, 920
23. Murani, A. P.: J. Magn. Magn. Mater., 1977, 5, 95
24. Murani, A. P.: Solid State Commun., 1977, 22, 25
25. Murani, A. P. and Heidemann, A.: Phys. Rev. Lett., 1978, 41, 1402
26. Murani, A. P.: Phys. Rev. Lett., 1978, 41, 1406
27. Mezei, F. and Murani, A. P.: J. Magn. Magn. Mater., 1979, 14, 211
28. Murani, A. P.: Solid State Commun., 1980, 33, 433
29. Murani, A. P.: J. Magn. Magn. Mater., 1981, 22, 271
30. Murani, A. P.: J. Phys. F: Met. Phys. 1985, 15, 417
31. Tsunoda, Y., Kunitomi, N., and Cable, J. W.: J. Appl. Phys., 1985, 57, 3753
32. Kaya, S. and Kussman, A.: Z. Physik, 1931, 72, 293
33. Piercy, G. R. and Morgan, E. R.: Can. J. Phys., 1953, 31, 529
34. Carr, W. J.: Phys. Rev., 1952, 85, 590
35. Sidorov, S. K. and Doroshenko, A. V.: Phys. Met. Metallogr., 1964, 18, 12
36. Cable, J. W. and Child, H. R.: Phys. Rev. B, 1974, 10, 4607
37. Kitaoka, Y., Ueno, K., and Asayama, K.: J. Phys. Soc. Japan, 1978, 44, 142
38. Aitken, R. G., Cheung, T. D., Kouvel, J. S., and Hurdequint, J.: J. Magn. Magn. Mat., 1982, 30, L1
39. Abdul-Razzaq, W. and Kouvel, J. S.: J. Appl. Phys., 1984, 55, 1623
40. Kouvel, J. S. and Abdul-Razzaq, W.: J. Magn. Magn. Mat., 1985, 53, 139

41. Hennion, B., Hennion, M., Hippert, F., and Murani, A. P.: J. Phys. F: Met. Phys., 1984, 14, 489
42. Cable, J. W., Nicklow, R. M., and Tsunoda, Y.: Phys. Rev. B, accepted for publication
43. Coles, B. R., Sarkissian, B. V. B., and Taylor, R. H.: Phil. Mag., 1978, 37, 489
44. Verbeek, B. H. and Mydosh, J. A.: J. Phys. F: Met. Phys., 1978, 8, L109
45. Monod, P. and Campbell, I. A.: Phys. Rev. Lett., 1984, 52, 2096
46. Brand, R. A. and Keune, W.: Phys. Rev. Lett., 1984, 52, 2097
47. Violet, C. E. and Borg, R. J.: Phys. Rev. Lett., 1984, 52, 2098
48. Lauer, J. and Keune, W.: Phys. Rev. Lett., 1982, 48, 1850
49. Varret, F., Hamzic, A., and Campbell, I. A.: Phys. Rev. B, 1982, 26, 5285
50. Campbell, I. A., Senoussi, S., Varret, F., Teillet, J., and Hamzic, A.: Phys. Rev. Lett., 1983, 50, 1615
51. Gabay, M. and Toulouse, G.: Phys. Rev. Lett., 1981, 47, 201
52. Dartyge, E., Bouchiat, H., and Monod, P.: Phys. Rev. B, 1982, 25, 6995
53. Beck, P. A.: Phys. Rev. B, 1985, 32, 7255
54. Cable, J. W., Parette, G., and Tsunoda, Y.: Phys. Rev. B, submitted for publication
55. Hamada, N.: J. Phys. Soc. Japan, 1981, 50, 77
56. Kakehashi, Y.: Phys. Rev. B., 1985, 32, 3035